European Journal of Medicinal Chemistry 44 (2009) 4585–4595

Contents lists available at ScienceDirect

European Journal of Medicinal Chemistry

journal homepage: http://www.elsevier.com/locate/ejmech

Original article

Synthesis, characterization, DNA binding properties and antioxidant activity of Ln(III) complexes with hesperetin-4-one-(benzoyl) hydrazone

Yong Li, Zheng-Yin Yang*, Ming-Fang Wang

College of Chemistry and Chemical Engineering and State Key Laboratory of Applied Organic Chemistry, Lanzhou University, Lanzhou 730000, PR China

ARTICLE INFO

Article history:
Received 9 April 2009
Received in revised form
25 June 2009
Accepted 25 June 2009
Available online 1 July 2009

Keywords:
Hesperetin hydrazone
Ln(III) complexes
DNA binding studies
Antioxidant activity

ABSTRACT

Novel Ln(III) complexes with hesperetin-4-one-(benzoyl) hydrazone (H_4L) have been synthesized and characterized. Electronic absorption spectroscopy, fluorescence spectra, ethidium bromide displacement experiments, iodide quenching experiments, salt effect and viscosity measurements indicate that the ligand and Ln(III) complexes, especially the Nd(III) complex, strongly bind to calf thymus DNA, presumably via an intercalation mechanism. The intrinsic binding constants of the Nd(III) complex and ligand with DNA were 2.39×10^6 and 2.70×10^5 M^{-1}, respectively. Furthermore, the antioxidant activity of the ligand and Ln(III) complexes was determined by superoxide and hydroxyl radical scavenging method in vitro, which indicate that the ligand and Ln(III) complexes have the activity to suppress $O_2^{-\bullet}$ and $HO^{\bullet}$ and the Ln(III) complexes exhibit more effective antioxidant activity than the ligand alone.

1. Introduction

It is well known that deoxyribonucleic acid (DNA) is an important genetic substance in organism. The regions of DNA involved vital processes, such as gene expression, gene transcription, mutagenesis and carcinogenesis [1]. Since DNA is an important cellular receptor, many chemicals exert their antitumor effects through binding to DNA thereby changing the republication of DNA and inhibiting the growth of the tumor cells, which is the basis of designing new and more efficient antitumor drugs and their effectiveness depends on the mode and affinity of the binding [2–5]. Therefore, the qualitative and quantitative analyses of the nucleic acids as the material base of genetic inheritance are becoming more and more important. Binding studies of small molecules to DNA are very important in the development of DNA molecular probes and new therapeutic reagents [6–8]. During the past decades, identifying small molecules that are capable of binding to DNA through an intercalation mode has attracted considerable interests [9]. Small molecule compounds would potentially be valuable tools in biotechnology, nanotechnology, therapeutic approaches and the study of nucleic acid conformations and then a large number of metal complexes with small molecule compounds as ligands are being used at the forefront of many of these efforts [10,11].

Some hydrazones and their metal complexes have diverse biological and pharmaceutical activities, such as antimicrobial, antituberculostatic, anticancer, antioxidant properties and so on [12–15]. Our previous studies indicate that naringenin hydrazones and their metal complexes possess better antitumor, antioxidant and cytotoxicity activities [16–18]. Furthermore, Schiff bases are an important class of ligands in coordination chemistry and are found to possess extensive applications in different fields, such as pharmacological field [19], which are able to inhibit the growth of several animal tumors [20]. Hesperetin (5,7,3′-trihydroxyl-4′-methoxyl-flavanone) is a kind of flavonoid which occurs ubiquitously in plants, fruits, flowers and foods of plant origin [21]. As an important bioactive Chinese traditional medicine, hesperetin has multiple biological and pharmacological activities, including antioxidant properties [22,23], inhibition of cancer development [24,25], effects on the blood-brain barrier [26,27], signal transduction pathways [28], etc. However, hesperetin hydrazones and their complexes have not been extensively investigated. Moreover, Our previous work clearly indicates that the lanthanide complexes possess better bioactivities, such as antioxidant activity, cytotoxic activity, DNA binding affinity and so on [16–18]. In addition, lanthanide ions are subjects of increasing interest in bioinorganic and coordination chemistry [29]. Lanthanide complexes with tetracycline, phenanthroline [30], adriamycin and pyridine [31,32] have been already synthesized as a probe to study nucleic acids.

In order to give a deep research to hesperetin ramifications and their lanthanide complexes, in this paper, we synthesized and characterized a novel ligand, hesperetin-4-one-(benzoyl) hydrazone

* Corresponding author. Tel.: +86 931 8913515; fax: +86 931 8912582.
E-mail address: yangzy@lzu.edu.cn (Z.-Y. Yang).

0223-5234/$ – see front matter © 2009 Elsevier Masson SAS. All rights reserved.
doi:10.1016/j.ejmech.2009.06.027

(H_4L, Fig. 1) and its Ln(III) complexes. We described a comparative study of the interaction of novel Ln(III) complexes and the ligand with calf thymus DNA (CT DNA) using electronic absorption spectroscopy, fluorescence spectra, ethidium bromide experiments, iodide quenching experiments, salt effect and viscosity measurements for the first time. The antioxidant activity of the ligand and its Ln(III) complexes was also investigated. Information obtained from our study would be helpful to understand the mechanism of interactions of hesperetin hydrazones and their complexes with nucleic acid and should be useful in the development of potential probes of DNA structure and conformation, and new therapeutic reagents for some certain diseases.

2. Results and discussion

2.1. Structure of the Ln(III) complexes

The complexes were prepared by direct reaction of ligand with the appropriate mole ratios of Ln(III) nitrate in acetone. The yields were good to moderate. The desired Ln(III) complexes were separated from the solution by suction filtration, purified by washing several times with ethanol. The complexes are air-stable for extended periods and soluble in DMSO and DMF; slightly soluble in ethanol and methanol; insoluble in benzene, water and diethyl ether. The molar conductivities of the complexes are around 73.9–88.1 S cm^2 mol^{-1} in DMF solution, showing that all complexes are 1:1 electrolytes [33]. The elemental analyses and molar conductivities show that formulas of the Ln(III) complexes conform to $[Ln(H_4L)_2(NO_3)_2]NO_3$ [Ln(III) = La, Sm, Dy, Yb and Nd].

The IR spectra of the complexes are similar. IR spectra usually provide a lot of valuable information on coordination reactions. All the spectra are characterized by vibrational bands mainly due to the NH, C═O, C═N and NO_3 groups. The ν (N–H) appears at 3362 cm^{-1} for the ligand, and this peak shifts at 3386 cm^{-1} or so for the complexes. The ν (C═O) vibration of the free ligand is at 1642 cm^{-1}; for the complexes, the peak shifts to 1610 cm^{-1}, $\Delta\nu_{(ligand-complexes)}$ is equal to 32 cm^{-1}. In the complexes, the band at 555 cm^{-1} or so is assigned to ν (M–O). It demonstrates that the oxygen of carbonyl has formed a coordinative bond with the lanthanide ions [34]. The band at 1604 cm^{-1} for the free ligand is assigned to the ν (C═N) stretch, which shifts to 1570 cm^{-1} for its complexes, $\Delta\nu_{(ligand-complexes)}$ is equal to 34 cm^{-1}. Weak bands at 410 cm^{-1} or so are assigned to ν (M–N) in the complexes. These shifts and new bands further confirm that the nitrogen of the imino-group bonds to the lanthanide ions [35]. The absorption bands of the coordinated nitrates were observed at about 1479 (ν_{as}) and 870 (ν_s) cm^{-1}. The ν_3 free nitrates appear at 1384 cm^{-1} or so in the spectra of the Ln(III) complexes. In addition, the separation of the two highest frequency bands $|\nu_4 - \nu_1|$ is approximately 160 cm^{-1}, and accordingly the coordinated NO_3^- ion in the complexes is a bidentate ligand [36].

The ^{1}H NMR spectra of the ligand and its La(III) complex are assigned as follows: H_4L (DMSO-d^6, 200 MHz), δ (ppm) 2.51 (1H, dd, J = 12.3, 17.0 Hz, 3(a)-H), 2.88 (1H, dd, J = 3.0, 17.0 Hz, 3(e)-H), 3.77 (3H, s, –OCH_3), 5.06 (1H, dd, J = 3.0, 12.3 Hz, 2-H), 5.87 (1H, d, J = 2.2 Hz, 6-H), 5.93 (1H, d, J = 2.2 Hz, 8-H), 6.93 (3H, br, 2′, 5′, 6′-H), 7.52 (2H, dd, J = 1.8, 7.4 Hz, 3″, 5″-H), 7.54 (1H, dd, J = 7.4, 11.6 Hz, 4″-H), 7.88 (2H, dd, J = 1.8, 11.6 Hz, 2″, 6″-H), 9.09 (1H, s, 3′-OH), 9.99 (1H, s, 7-OH), 11.12 (1H, s, –NH–C═O), 13.06 (1H, s, 5-OH). $[Ln(H_4L)_2(NO_3)_2]NO_3$: (DMSO-d^6, 200 MHz), δ (ppm) 2.74 (2H, dd, J = 8.0, 16.2 Hz, 3(a)-H), 2.90 (2H, dd, J = 2.2, 16.2 Hz, 3(e)-H), 3.85 (6H, s, –OCH_3), 5.50 (2H, dd, J = 2.2, 8.0 Hz, 2-H), 5.58 (2H, d, J = 2.2 Hz, 6-H), 5.87 (2H, d, J = 2.2 Hz, 8-H), 6.92 (6H, br, 2′, 5′, 6′-H), 7.45 (4H, dd, J = 2.0, 7.6 Hz, 3″, 5″-H), 7.85 (2H, dd, J = 7.6, 13.4 Hz, 4″-H), 7.96 (4H, dd, J = 2.0, 13.4 Hz, 2″, 6″-H), 9.06 (2H, s, 3′-OH), 10.00 (2H, s, 7-OH), 11.12 (2H, s, –NH–C═O), 13.07 (2H, s, 5-OH). In the complex, the –OH-5 hydrogen still exists. The hydrogen of the ═NNH– group is also detected and there are no hydrogens replaced by the metal ion, which is also supported by the IR spectra.

The complexes begin to decompose at 298 °C or so and there are three exothermic peaks appear around 298–646 °C. The corresponding TG curves show a series of weight loss. Under 200 °C, there are no endothermic peaks and no weight loss on the corresponding curves. It indicates that there are no crystal or coordinate solvent molecules. While being hated to 800 °C, the complexes become their corresponding oxides and the residues are in accordance with calculations.

The study of the electronic spectra in the ultraviolet and visible (UV–vis) ranges for the Ln(III) complexes and ligand was carried out in Tris–HCl buffer solution. The electronic spectra of the free ligand have a strong band at λ_{max} = 328 nm and a medium band at λ_{max} = 285 nm. The complexes also yield two bands, and the two bands are shifted to 343 and 291 nm or so. These indicate that the Ln(III) complexes are formed.

The electrospray ionization (ESI) mass spectra of Sm(III) and Dy(III) complexes were made. The mass spectra of Sm(III) and Dy(III) complexes show peaks at 991 and 1002 which can be assigned to the fragments [Sm(III) complex–$3NO_3$–H]$^{2+}$ and [Dy(III) complex–$3NO_3$–2H]$^+$, respectively.

Since the crystal structures of the Ln(III) complexes have not been obtained yet, we characterized the complexes and determined its possible structure by elemental analyses, molar conductivities, IR spectra, ^{1}H NMR, TG/DTA, mass spectra and UV–vis spectra. The ligand and lanthanide ions can form mononuclear ten-coordination $[Ln(H_4L)_2(NO_3)_2]NO_3$ [Ln(III) = La, Sm, Dy, Yb and Nd] complexes with 1:2 metal-to-ligand stoichiometry at the Ln(III) centers (Fig. 2).

2.2. Magnetic properties

Effective magnetic moments were calculated from the molar magnetic susceptibilities [49]. Dy(III) complex ($\Delta\nu$ = 42.0 Hz) has a magnetic moment of 12.60 B.M., as predicted for a high spin f^9 system with five unpaired electrons. However, La(III) complex ($\Delta\nu$ = 0) is diamagnetic as expected for a f^0 configuration. Magnetic moments for Nd(III) complex ($\Delta\nu$ = 4.5 Hz), Sm(III) complex ($\Delta\nu$ = 1.5 Hz) and Yb(III) complex ($\Delta\nu$ = 7.2 Hz) are 0, 3.84, 1.85 and 4.65 B.M., respectively. These results are consistent with the calculated values.

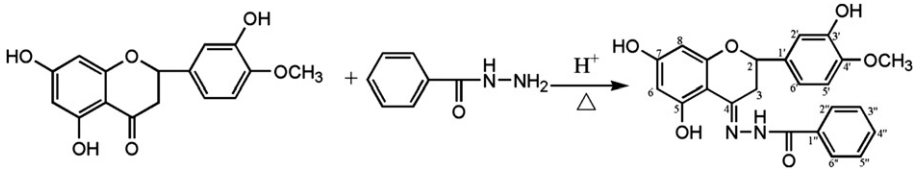

Fig. 1. Scheme of the synthesis of the ligand (H_4L).

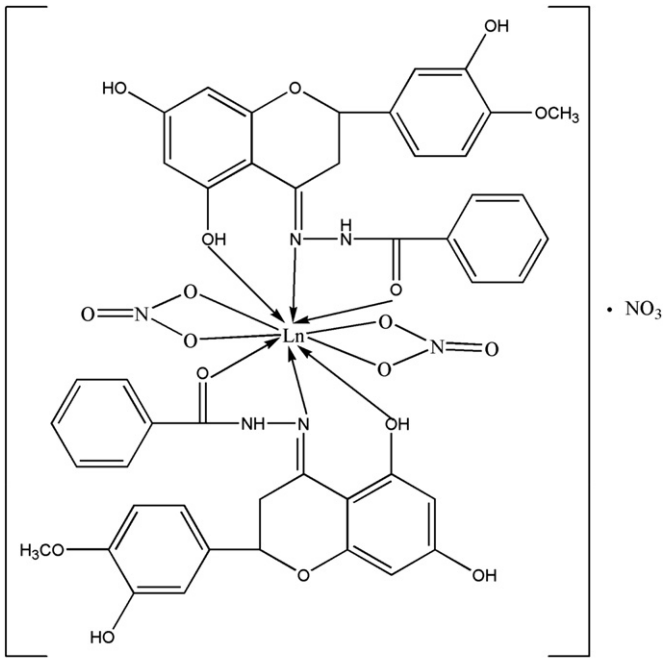

(Ln = La, Sm, Dy, Yb and Nd)

Fig. 2. The suggested structure of the lanthanide complexes.

2.3. DNA binding studies

2.3.1. Electronic absorption titration

Before reacting the ligand and its Ln(III) complexes interacting with CT DNA, its solution behavior in Tris–HCl buffer solution at room temperature was monitored by UV–vis spectroscopy for 24 h. Liberation of the ligand and its Ln(III) complexes was not observed under these conditions. These suggest that the ligand and its Ln(III) complexes are stable under the conditions studied.

The electronic absorption spectra of the free ligand and Nd(III) complex in the absence and presence of CT DNA are given in Fig. 3. As seen from Fig. 3a, there exist two bands at 328 and 285 nm for the free ligand, and in Fig. 3b two bands are at 343 and 291 nm for the Nd(III) complex. With increasing concentrations of CT DNA, the absorption bands of the free ligand at 328 and 285 nm exhibited hypochromism of 40.0% and 32.6%, respectively. For the Nd(III) complex, the absorption bands at 343 and 291 nm appeared with hypochromism of 33.7% and 38.0%. The hypochromisms observed for the bands of the free ligand and its Nd(III) complex are accompanied by a small red shift by less than 4 nm.

The electronic absorption spectroscopy is one of the most useful techniques in DNA binding studies of metal complexes [37]. A compound binding to DNA through intercalation usually results in hypochromism and bathochromism due to the intercalation mode involving a strong π–π stacking interaction between the aromatic chromophore and the DNA base pairs. It seems to be generally accepted that the extent of the hypochromism in the UV–vis band is consistent with the strength of intercalative interaction [38]. So the above phenomena imply that the compounds interact with CT DNA quite probably by intercalating the compounds into the DNA base pairs. From the results of electronic absorption spectroscopy, we can conclude that the free ligand and Nd(III) complex can interact with CT DNA through the same mode (intercalation).

In order to further test if the complexes could bind to CT DNA via the mode of intercalation, ethidium bromide (EB) was employed, because EB interacts with DNA as a typical indicator of intercalation [39]. Fig. 4 shows the electronic absorption spectra when EB was employed. The absorbance of Tris–HCl buffer solution is highest when there is only EB alone. After adding CT DNA into Tris–HCl buffer solution, the absorbance decreases. However, it increases when the ligand and Nd(III) complex was added dropwise into the buffer solution. Fig. 4 shows that the maximal absorption of EB at 479 nm decreased and shifted to 494 nm in the presence of DNA, which was characteristic of intercalation mode. Curve (B) in Fig. 4 was the absorption of a mixture solution of EB, DNA and the free ligand or Nd(III) complex. It was found that the absorption at 495 nm increased comparing with curve (C). It could result from two reasons: (1) EB bound to the free ligand or Nd(III) complex strongly, resulting in the decreased amount of EB intercalated into DNA; (2) there exists a competitive intercalation between the free ligand or Nd(III) complex and EB with DNA, so releasing some free EB from DNA–EB system. However, the former reason could be precluded because there were no new absorption peaks appearing.

2.3.2. Fluorescence spectra

The ligand and its Ln(III) complexes can emit weak luminescence in Tris–HCl buffer with a max wavelength of about 445 nm. The results of the emission titrations for the Nd(III) complex and free ligand with DNA are illustrated in the titration curves (Fig. 5).

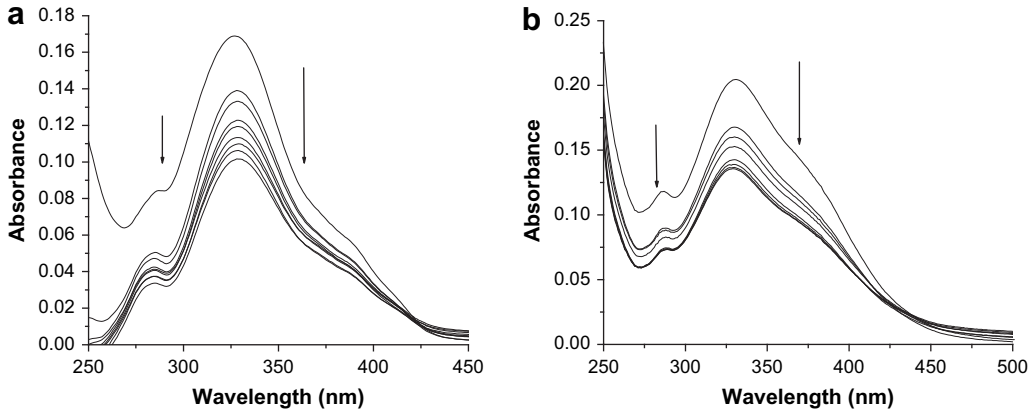

Fig. 3. (a) Electronic absorption spectra of the free ligand (10 μM) in the absence (top spectrum) and presence of increasing amounts of CT DNA (2.5, 5.0, 7.5, 10.0, 12.5, 15.0, 17.5 and 20.0 μM; subsequent spectra). Arrow shows the absorbance changes upon increasing DNA concentration. (b) Electronic absorption spectra of the Nd(III) complex (10 μM) in the absence (top spectrum) and presence of increasing amounts of CT DNA (2.5, 5.0, 7.5, 10.0, 12.5, 15.0, 17.5 and 20.0 μM; subsequent spectra). Arrow shows the absorbance changes upon increasing DNA concentration.

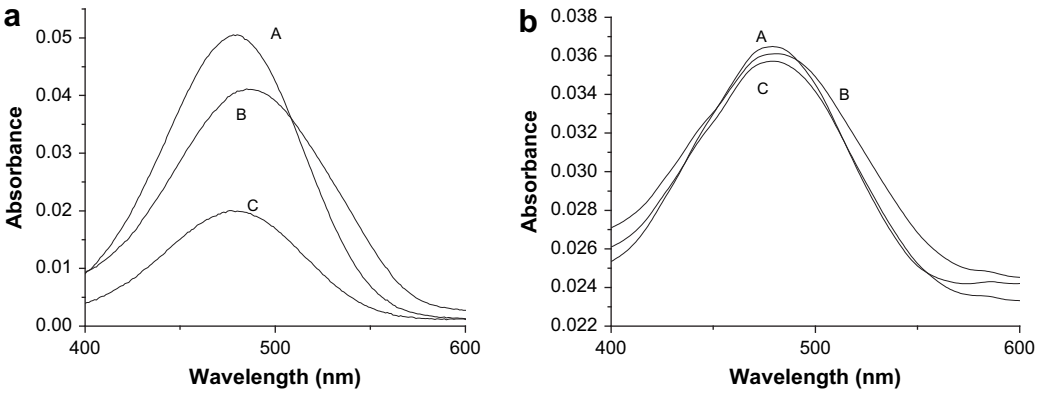

Fig. 4. (a) The visible absorption spectra of 1×10^{-5} M EB (A); (A) + 2.5×10^{-5} M DNA (C); (C) + 2.5×10^{-5} M free ligand (B) in Tris–HCl buffer (5 mM tris–HCl, 50 mM NaCl, pH 7.1) solution. (b) The visible absorption spectra of 1×10^{-5} M EB (A); (A) + 2.5×10^{-5} M DNA (C); (C) + 2.5×10^{-5} M Nd(III) complex (B) in Tris–HCl buffer (5 mM tris–HCl, 50 mM NaCl, pH 7.1) solution.

Compared to the Nd(III) complex and free ligand alone, the emission intensity increases with increasing concentrations of CT DNA.

The results of the emission titrations suggest that both the Nd(III) complex and free ligand are protected from solvent water molecules by the hydrophobic environment inside the DNA helix and that the Nd(III) complex can be protected more efficiently than the free ligand. This implies that both the Nd(III) complex and free ligand can insert between DNA base pairs deeply and the Nd(III) complex can bind to DNA more strongly than the free ligand. Since the hydrophobic environment inside the DNA helix reduces the accessibility of solvent water molecules to the compound and the compound mobility is restricted at the certain binding sites, a decrease of the vibrational modes of relaxation results. The binding of the compounds to DNA leading to a significantly increase in emission intensity also agrees with those observed for other intercalators [40]. According to the Scatchard equation, a plot of r/C_f

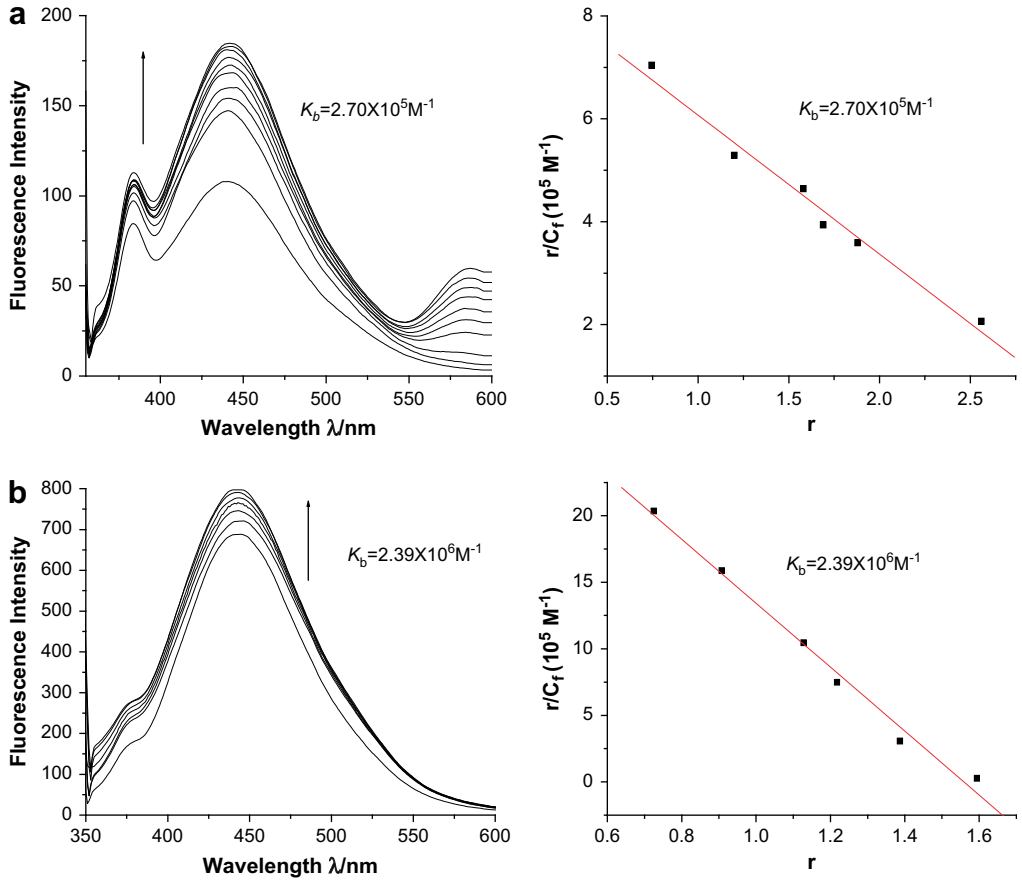

Fig. 5. (a) The emission enhancement spectra of free ligand (10 μM) in the presence of 0, 2.5, 5, 7.5, 10, 12.5 and 15 μM DNA. Arrow shows the emission intensity changes upon increasing DNA concentration. *Inset*: Scatchard plot of the fluorescence titration data of ligand, $K_b = 2.70 \times 10^5$ M^{-1}. (b) The emission enhancement spectra of Nd(III) complex (10 μM) in the presence of 0, 2.5, 5, 7.5, 10, 12.5 and 15 μM DNA. *Inset*: Scatchard plot of the fluorescence titration data of ligand, $K_b = 2.39 \times 10^6$ M^{-1}.

versus r gave the binding constants (K_b) 2.39×10^6 and 2.70×10^5 M^{-1} from the fluorescence data for the Nd(III) complex and the free ligand, respectively. K_b values for the La(III) complex, Sm(III) complex, Dy(III) complex and Yb(III) complex were 3.23×10^5, 1.65×10^6, 9.66×10^5 and 1.25×10^6 M^{-1}, respectively, which were obtained according to the same method. These results show that the ligand and its Ln(III) complexes can bind to DNA, especially the Nd(III) complex binds more strongly than the free ligand. The higher binding affinity of the Nd(III) complex is probably attributed to the extension of the π system of the intercalated ligand and the coordination of Nd(III), which leads to a planar area greater than that of the free ligand and that the coordinated ligand penetrates more deeply into and stacks more strongly with DNA base pairs.

The DNA binding modes of the compounds were further monitored by a fluorescent EB displacement assay. It is well known that EB can intercalate nonspecifically into DNA which causes it to fluoresce strongly. Competitive binding of other drugs to DNA and EB will result in displacement of DNA and a decrease in the fluorescence intensity. The fluorescence-based competition technique can provide indirect evidence for the DNA binding mode. The emission band of the DNA–EB system decreased in intensity with an increase of the compounds concentrations, indicating that the compounds can displace EB from DNA–EB system [41]. Such characteristic change is usually observed in intercalative DNA interactions [42]. Steady-state emission quenching experiments are used to observe the binding mode of the Nd(III) complex and free ligand to CT DNA. Fig. 6 shows the emission spectra of the DNA–EB system with increasing amounts of the Nd(III) complex and free ligand. The addition of the Nd(III) complex and free ligand to the DNA-bound EB solutions caused marked reduction in emission intensities. The quenching plots illustrated that the quenching of EB bound to DNA by the complexes and free ligand is in good agreement with the linear Stern–Volmer equation. In the plots of F_0/F versus [Q], K_q is given by the ratio of the slope to the intercept. The K_q values for the Nd(III) complex and ligand are 1.20×10^5 and 4.73×10^4 M^{-1}, respectively. K_q values for the La(III) complex, Sm(III) complex, Dy(III) complex and Yb(III) complex were 6.67×10^4, 1.17×10^5, 1.09×10^5 and 1.11×10^5 M^{-1}, respectively, which were obtained according to the same method. The data show that the interaction of the Ln(III) complexes with DNA is stronger than that of the free ligand, which is consistent with the electronic absorption spectral results. Since these changes indicate only one kind of quenching process, it may be concluded that the Ln(III) complexes and free ligand bind to DNA via the same mode (intercalation mode).

2.3.3. Iodide quenching experiments

The results of the emission titrations for the Nd(III) complex and potassium iodide with absence and presence of CT DNA are illustrated in the titration curves (Fig. 7). Compared to the Nd(III) complex alone, the emission intensity decreases with increasing concentrations of CT DNA. The quenching plots illustrated that the quenching studies of the Nd(III) complex are in good agreement with the linear Stern–Volmer equation.

In the aqueous solution, iodide and ferrocyanide anions quench the fluorescence of Nd(III) complex very efficiently, so we used potassium iodide as the quencher to determine the relative accessibilities of the free and bound Nd(III) complexes. From Fig. 7,

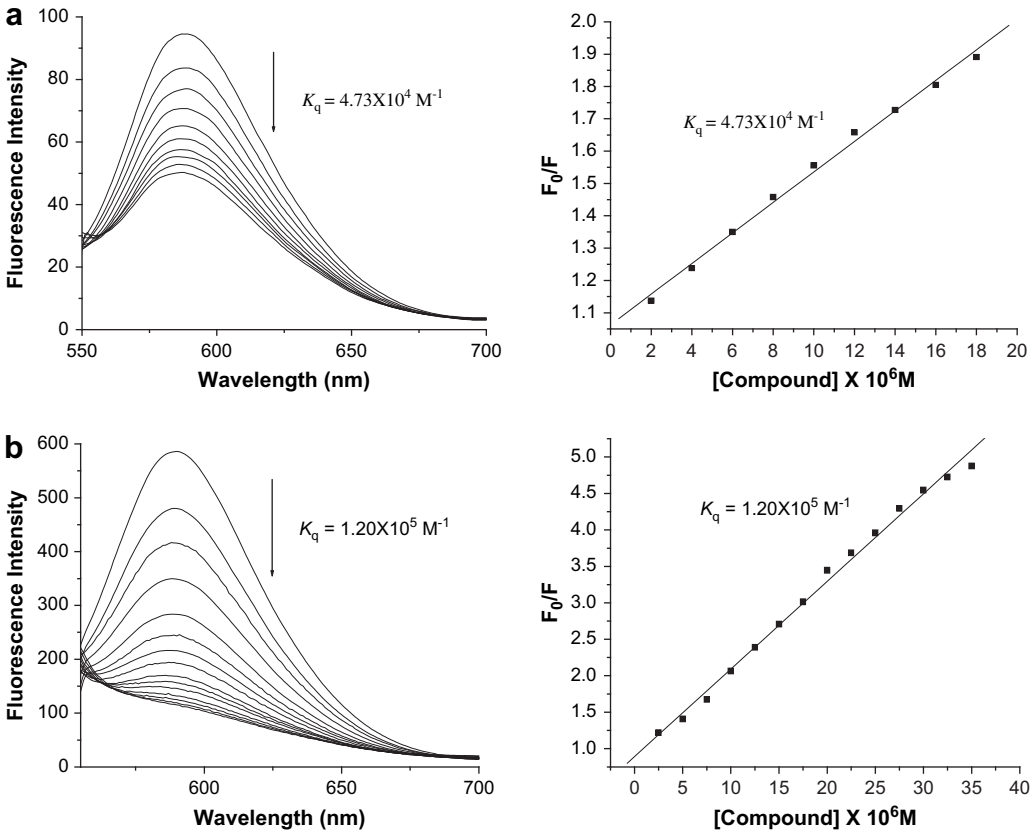

Fig. 6. (a) The emission spectra of DNA–EB system, in the presence of 0, 2.5, 5, 7.5, 10, 12.5, 15, 17.5, 20 and 22.5 μM ligand. Arrow shows the emission intensity changes upon increasing ligand. *Inset*: Stern–Volmer plot of the fluorescence titration data of ligand. $K_q = 4.73 \times 10^4$ M^{-1}. (b) The emission spectra of DNA–EB system, in the presence of 0, 2.5, 5, 7.5, 10, 12.5, 15, 17.5, 20, 22.5, 25, 27.5, 30, 32.5 and 35 μM Nd(III) complex. Arrow shows the emission intensity changes upon increasing Nd(III) complex. *Inset*: Stern–Volmer plot of the fluorescence titration data of Nd(III) complex. $K_q = 1.20 \times 10^5$ M^{-1}.

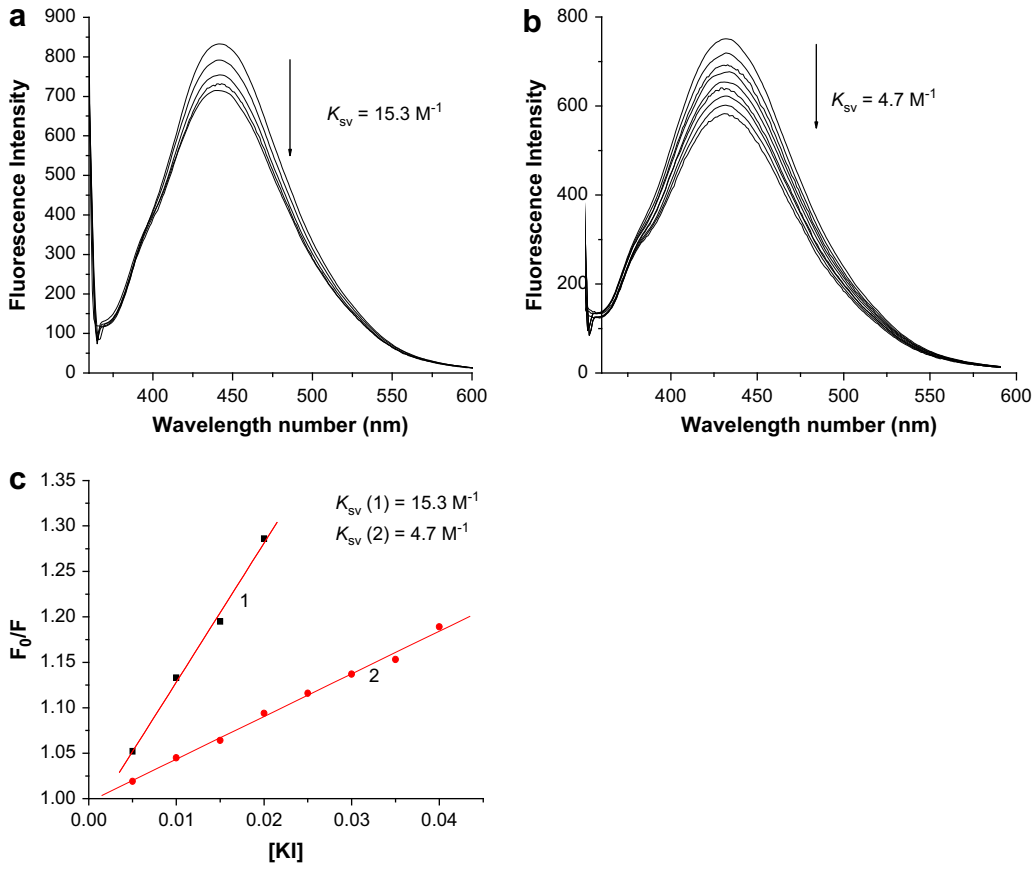

Fig. 7. (a) Fluorescence spectra of Nd(III) complex (10 μM) with increasing concentration of KI (5, 10, 20, 30, 40, 50, 60, 70 and 80 mM). (b) Fluorescence spectra of Nd(III) complex (10 μM) and DNA (20 μM) system with increasing concentration of KI (5, 10, 20, 30, 40, 50, 60, 70 and 80 mM). (c) *Inset*: Stern–Volmer plot of the fluorescence titration data of Nd(III) complex. Effect of KI concentration (1: Nd(III) complex + KI; 2: Nd(III) complex + KI + CT DNA). K_{sv} (1) = 15.3 M^{-1}, K_{sv} (2) = 4.7 M^{-1}.

we can find that the addition of Nd(III) complex and CT DNA results in extensive quenching of the fluorescence intensity. The quenching data were plotted according to the Stern–Volmer equation and the slopes were calculated by the linear least-squares method. The observed quenching constants were 15.3 and 4.7 M^{-1} with and without CT DNA, respectively. The quenching of the Nd(III) complex was in fact enhanced by a factor of more than 3 when the Nd(III) complex was bound to the DNA helix. We can conclude that the

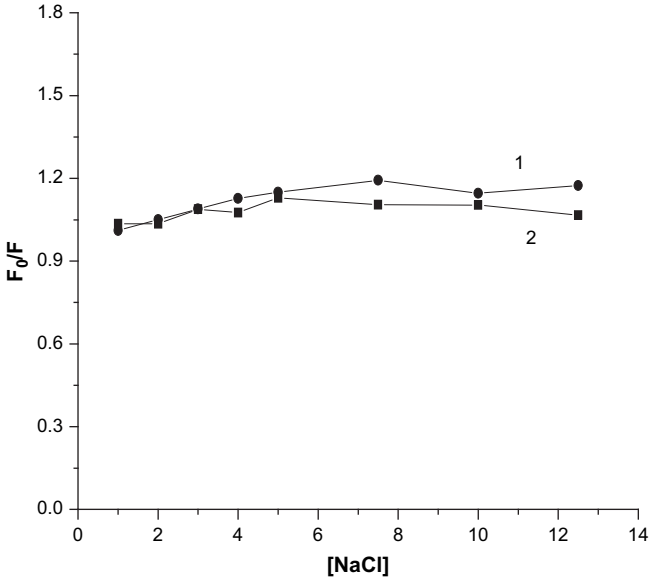

Fig. 8. Effect of NaCl concentration (1: Nd(III) complex + NaCl; 2: Nd(III) complex + NaCl + CT DNA).

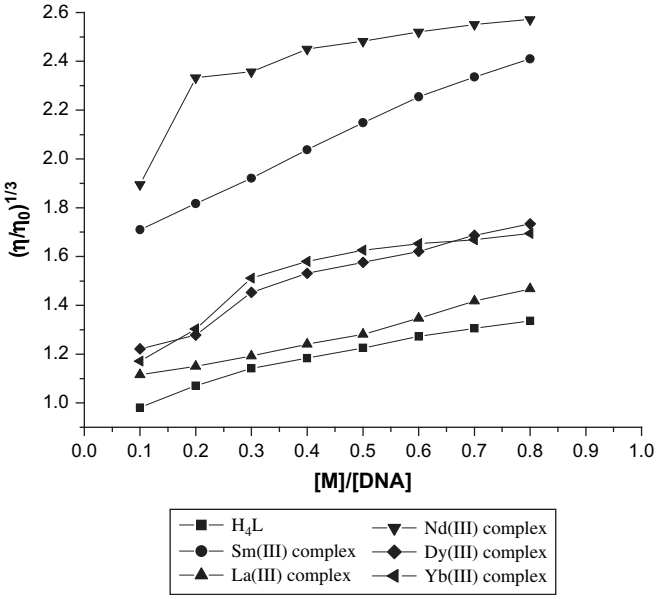

Fig. 9. Effect of increasing amounts of the ligand and its Ln(III) complexes on the relative viscosity of DNA at 25.0 °C.

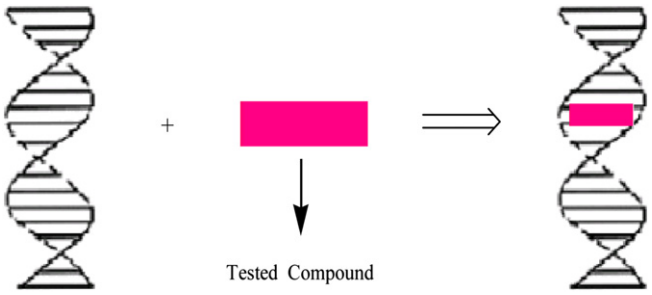

Fig. 10. Molecular mode for Ln(III) complexes (in an intercalative mode).

Ln(III) complexes are intercalated into the DNA helix and they should be protected from the anionic quencher, owning to the base pairs above and below the intercalators [43].

2.3.4. Salt effect

The effect of the ionic strength on the compounds fluorescence was tested by the addition of a strong electrolyte, NaCl. As seen from Fig. 8, there are almost no changes happening to the fluorescence emission intensities with increasing concentrations of CT DNA.

The effect of the ionic strength on the Nd(III) complex fluorescence intensity was tested by the addition of a strong electrolyte, such as NaCl, instead of potassium iodide. Cations of the salts can neutralize the negatively charged phosphate. If the compound binds to DNA through an electrostatic interaction mode, the surface of DNA will be surrounded by the sodium ions with the increase of ionic strength. Then the compound is difficult to approach DNA and the strength of interaction with DNA decreases, the degree of fluorescence quenching also falls [44]. Addition of NaCl to the Nd(III) complex in the absence and presence of CT DNA has little or no influence on the fluorescence intensity, showing that the interaction of the Nd(III) complex with CT DNA is not electrostatic interaction.

2.3.5. Viscosity measurements

In order to further clarify the interaction nature between the compounds and DNA, viscosity measurements were carried into execution. Optical photophysical probes provide necessary but not sufficient evidence to support a binding mode. Hydrodynamic measurements that are sensitive to length change (i.e. viscosity and sedimentation) are regarded as the least ambiguous and the most critical tests of a binding mode in solution in the absence of crystallographic structural data [45]. A classical intercalation mode demands that the DNA helix must lengthen as base pairs are separated to accommodate the binding complexes, leading to the increase of DNA viscosity, as for the behaviors of the known DNA intercalators [38]. In contrast, a partial and/or non-classical intercalation of the complex could bend (or kink) the DNA helix, reducing its viscosity concomitantly [45]. In addition, some complexes such as $[Ru(bpy)_3]^{2+}$, which interacts with DNA by an electrostatic binding mode, have no influence on DNA viscosity [46]. The effects of all the compounds on the viscosity of CT DNA are shown in Fig. 9. The viscosities of the DNA increase steadily with increasing concentrations of ligand and Ln(III) complexes and the extent of the increase observed for the ligand is smaller than that for the Ln(III) complexes with an increasing concentration of the complexes. Viscosity measurements clearly show that all the compounds can intercalate between adjacent DNA base pairs, causing an extension in the helix and thus increase the viscosity of DNA, and that the complexes can intercalate more strongly and deeply than the free ligand, leading to the greater increase in viscosity of the DNA. The results obtained from the viscosity experiments validate those obtained from the spectroscopic studies.

On the basis of all the spectroscopic studies together with the viscosity measurements, we find that the Ln(III) complexes and free ligand can bind to CT DNA via an intercalative mode (Fig. 10) and the Ln(III) complexes bind to CT DNA more strongly and deeply than the free ligand.

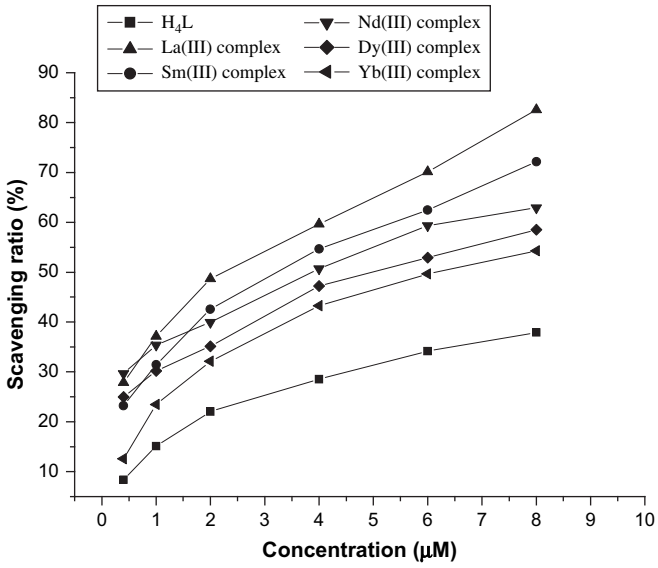

Fig. 11. Scavenging effect of the ligand and Ln(III) complexes on $O_2^{-\bullet}$.

2.4. Antioxidant activity

Owning to the ligand and its Ln(III) complexes exhibit good DNA binding affinity, it is considered worthwhile to study the antioxidant activity of these compounds. The antioxidant properties of hesperetin derivatives have attracted a lot of interests and have been extensively investigated, mainly in the in vitro systems [21,22].

Table 1
The influence of investigated compounds for $O_2^{-\bullet}$.

Compound	Average inhibition (%) for $O_2^{-\bullet}$ (μM)						Equation	IC_{50} (μM)	R^2
	0.4	1.0	2.0	4.0	6.0	8.0			
H_4L	8.41	15.11	22.06	28.54	34.17	37.89	$y = 22.67x + 16.10$	31.287	0.989
La(III) complex	27.85	37.14	48.71	59.62	70.14	82.54	$y = 40.30x + 39.65$	1.806	0.955
Sm(III) complex	23.25	31.46	42.59	54.67	62.43	72.14	$y = 37.06x + 34.25$	2.661	0.970
Nd(III) complex	29.67	35.42	39.97	50.72	59.36	62.91	$y = 26.25x + 36.78$	3.189	0.945
Dy(III) complex	24.98	30.22	35.13	47.21	52.89	58.52	$y = 26.17x + 31.96$	4.890	0.948
Yb(III) complex	12.59	23.46	32.13	43.25	49.67	54.28	$y = 32.28x + 24.14$	6.236	0.995

IC_{50} values were calculated from regression lines where: x was log of the tested compound concentration and y was percent inhibition of the tested compounds. When the percent inhibition of the tested compounds was 50%, the tested compound concentration was IC_{50}. R^2 = correlation coefficient.

Table 2
The influence of investigated compounds for HO•.

Compound	Average inhibition (%) for HO• (μM)						Equation	IC_{50} (μM)	R^2
	1.0	2.0	3.0	4.0	5.0	6.0			
H_4L	1.17	8.61	14.03	17.54	21.05	23.79	$y = 29.06x + 0.52$	50.429	0.995
La(III) complex	20.03	50.38	64.66	72.18	81.95	92.53	$y = 88.97x + 21.30$	2.102	0.994
Sm(III) complex	23.31	33.08	48.87	57.14	65.41	74.26	$y = 66.00x + 18.92$	2.957	0.961
Nd(III) complex	18.80	30.01	39.30	48.50	57.14	61.20	$y = 55.88x + 15.88$	4.079	0.973
Dy(III) complex	13.53	23.35	32.25	40.12	48.14	54.63	$y = 52.56x + 10.31$	5.690	0.963
Yb(III) complex	6.83	18.03	25.22	35.43	42.01	51.53	$y = 55.51x + 3.41$	6.907	0.952
Mannitol	2.30	12.52	24.63	32.91	43.09	43.82	$y = 57.26x - 0.73$	10.190	0.958

IC_{50} values were calculated from regression lines where: x was log of the tested compound concentration and y was percent inhibition of the tested compounds. When the percent inhibition of the tested compounds was 50%, the tested compound concentration was IC_{50}. R^2 = correlation coefficient.

Their free radical scavenging ability is always excellently directed toward superoxide radical ($O_2^{-\bullet}$) and hydroxyl radical (HO•) which are highly reactive products of reactive oxygen species (ROS) implicated with pathogenic processes including carcinogenesis through direct effects on DNA directly and by acting as a tumor promoter [47]. In this paper, the antioxidant activity of the ligand and its Ln(III) complexes was studied by comparing their scavenging effects on superoxide radical ($O_2^{-\bullet}$) and hydroxyl radical (HO•) in KH_2PO_4–Na_2HPO_4 buffer solution.

The data of the suppression ratio for $O_2^{-\bullet}$ are listed in Table 1. We find that the inhibitory effect of the compounds tested on $O_2^{-\bullet}$ is concentration dependent and the suppression ratio increases with increasing sample concentrations in the range tested (Fig. 11). The average suppression ratio of the free ligand ($IC_{50} = 31.287$ μM) for $O_2^{-\bullet}$ is the least in all compounds. The La(III) complex ($IC_{50} = 1.806$ μM) is the most effective in the five lanthanide complexes and the Nd(III) complex ($IC_{50} = 3.189$ μM) is also a more effective inhibitor than the free ligand.

The data of the suppression ratio for HO• are listed in Table 2. We find that the inhibitory effect of the compounds tested on HO• is also concentration dependent and the suppression ratio increases with increasing sample concentrations in the range tested (Fig. 12). The average suppression ratio of the free ligand ($IC_{50} = 50.429$ μM) for HO• is the least and the La(III) complex ($IC_{50} = 2.102$ μM) is the most effective in all the compounds. The order of the suppression ratio of the tested compounds for HO• is La(III) complex > Sm(III) complex > Nd(III) complex > Dy(III) complex > Yb(III) complex > mannitol > H_4L.

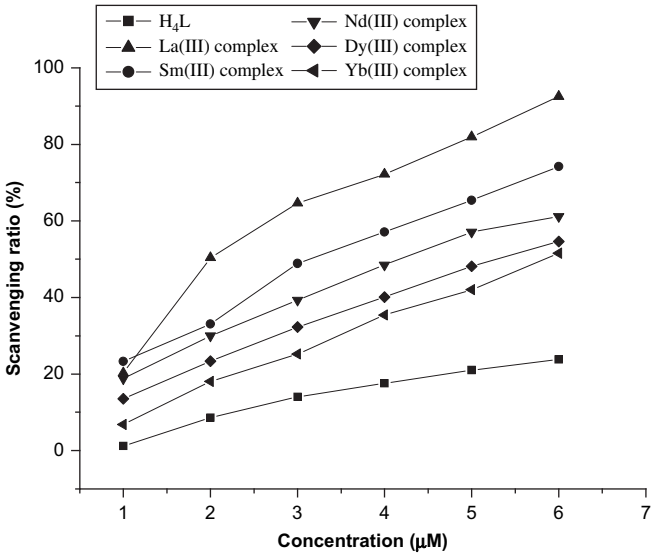

Fig. 12. Scavenging effect of the ligand and Ln(III) complexes on HO•.

From Tables 1 and 2, we can easily find that lanthanide complexes exhibit considerable scavenging activity due to the chelation of organic molecules to the lanthanide ions which exert different and selective effects on scavenging radicals of the biological system. We also find that the five lanthanide complexes are more effective inhibitor than mannitol which is usually used as special scavenger for HO•. It is reported that IC_{50} value of ascorbic acid (Vc, a standard agent for non-enzymatic reaction) for HO• is 1.537 mg mL^{-1} (8.727 mmol), and the scavenging effect for $O_2^{-\bullet}$ is only 25% at 1.75 mg mL^{-1} (9.94 mmol) [48]. Notably, the investigated ligand and lanthanide complexes have much stronger scavenging abilities for HO• and $O_2^{-\bullet}$ radicals. It was believed that the information obtained form present work would be useful to develop new potential antioxidants and therapeutic agents for some diseases.

3. Conclusion

Taken together, a novel hesperetin Schiff base ligand, hesperetin-4-one-(benzoyl) hydrazone (H_4L), and its La(III), Sm(III), Nd(III), Dy(III) and Yb(III) complexes were reported. The structure of the Ln(III) complexes was determined on the basis of elemental analyses, molar conductivities, IR spectra, ^1H NMR, TG/DTA, mass spectra and UV–vis spectra. It is notable that the ligand and its Ln(III) complexes have good planar property, which results in the higher DNA binding constants of compounds. Experimental results indicate that the ligand and lanthanide complexes bind to DNA via an intercalation mode and the lanthanide complexes can bind to DNA more strongly than the free ligand alone. Moreover, lanthanide complexes have better antioxidant activity than the ligand. Results obtained from our present work would be useful to understand the mechanism of interactions of the small molecule compounds binding to DNA and helpful in the development of their potential biological, pharmaceutical and physiological implications in the future.

4. Experimental

4.1. Materials

Nitroblue tetrazolium (NBT), methionine (MET), vitamin B_2 ($VitB_2$), EB and CT DNA were purchased from Sigma Chemical Co. Ethylenediaminetetraaceticacid (EDTA), safranin, benzoyl hydrazine, acetic acid, hesperetin, NaCl, potassium iodide, $Ln(NO_3)_3 \cdot 6H_2O$ [Ln(III) = La, Sm, Dy, Yb and Nd] were produced in China. All chemicals used were of analytical grade. EDTA–Fe(II) and KH_2PO_4–Na_2HPO_4 buffers were prepared with doubly distilled water.

All the experiments involved with the interaction of the ligand and its lanthanide complexes with CT DNA were carried out in doubly distilled water buffer containing 5 mM Tris [Tris(hydroxymethyl)-aminomethane] and 50 mM NaCl and adjusted to pH 7.1 with

hydrochloric acid. Solution of CT DNA in Tris–HCl buffer gave ratios of UV absorbance of about 1.8–1.9:1 at 260 and 280 nm, indicating that the CT DNA was sufficiently free of protein [22]. The CT DNA concentration per nucleotide was determined spectrophotometrically by employing an extinction coefficient of 6600 $M^{-1}\,cm^{-1}$ at 260 nm [23]. The ligand and its complexes were dissolved in a solvent mixture of 1% DMF and 99% Tris–HCl buffer (pH 7.1) at the concentration 1.0×10^{-5} M.

4.2. Instrumentation

Carbon, hydrogen and nitrogen were determined using an Elemental Vario EL analyzer. The metal contents of the complexes were determined by titration with EDTA (xylenol orange tetrasodium salt used as an indicator and hexamethylenetetramine as buffer). The melting point of the ligand was determined on a Beijing XT4-100X microscopic melting point apparatus (the thermometer was not corrected). The IR spectra were obtained in KBr discs on a Therrno Mattson FTIR spectrophotometer in the 4000–400 cm^{-1} region. ^1H NMR spectra were recorded on a Varian VR 200 MHz spectrometer in DMSO-d^6 with TMS (tetramethylsilane) as internal standard. Mass spectra were performed on an APEX II FT-ICR MS instrument using methanol as mobile phase. All conductivity measurements were performed in DMF solution with a DDS-11C conductometer at 25.0 °C. Thermal behavior (TG/DTA) was monitored on a PCT-2 differential thermal analyzer. The UV–vis spectra were recorded on a Shimadzu UV-240 spectrophotometer. Fluorescence measurements were recorded on a Hitachi RF-4500 spectrofluorophotometer at room temperature. Magnetic susceptibility was determined in deuterium oxide solution (2% *t*-butyl alcohol) at 305 K by JEOL PMX-60SI NMR spectrometer (Japan) according to the literature method [49]. The antioxidant activity was performed in DMF solution with a 721-E spectrophotometer.

4.3. Preparation of ligand (H_4L)

Scheme of the synthesis of the ligand is shown in Fig. 1. Hesperetin (3.02 g, 10 mmol) and benzoyl hydrazine (1.50 g, 11 mmol) were dissolved in methanol (40 mL). Acetic acid (1.0 mL) was added to this solution and the solution was refluxed on a water bath for one day with stirring. After that, the brown solution was concentrated and cooled, a grey solid separating out and the grey precipitate was filtered, washed with massive water, and recrystallized from DMF and water to give the ligand. Yield: 72.14%. Mp 264–266 °C. Anal Calcd. for $C_{23}H_{20}N_2O_6$ requires C, 65.71; H, 4.79; N, 6.66. Found: C, 65.51; H, 4.92; N, 6.76. IR ν_{max} (cm^{-1}): ν (C=O): 1642, ν (C=N): 1605, ν (N–H): 3362 cm^{-1}. λ_{max} (nm): 328, 285 nm.

4.4. Preparation of Ln(III) complexes

The H_4L ligand (84 mg, 0.20 mmol) was dissolved in acetone (20 mL). After 5 min, La(III) nitrate (87 mg, 0.20 mmol) was added quickly and the solution was refluxed on a water bath for 10 h with stirring. A yellow precipitate, the La(III) complex, was separated from the solution by suction filtration, purified by washing several times with ethanol and dried for 24 h in a vacuum. The Sm(III), Dy(III), Yb(III) and Nd(III) complexes were prepared by the same way. Anal Calcd. for La(III) complex $C_{46}H_{40}N_7O_{21}La$ requires: C, 47.39; H, 3.46; N, 8.41; La, 11.92; Found: C, 47.48; H, 3.29; N, 8.43; La, 11.94. IR ν_{max} (cm^{-1}): ν (C=O): 1610, ν (C=N): 1561, ν (N–H): 3384, ν (NO_3): 1479, 1384, 1314, 1189, 707 cm^{-1}. λ_{max} (nm): 287, 333 cm^{-1}. Λ_m (S cm^2 mol^{-1}): 82.1. Thermal analyses: $T_{Decomp.}$ (°C): 298, 308, 646. Residue Calcd. (%) 13.82 (13.98). Anal Calcd. for Sm(III) complex $C_{46}H_{40}N_7O_{21}Sm$ requires: C, 46.93; H, 3.42; N, 8.33; Sm, 12.77; Found: C, 47.08; H, 3.39; N, 8.43; Sm, 12.94. IR ν_{max} (cm^{-1}): ν (C=O): 1608, ν (C=N): 1569, ν (N–H): 3382, ν (NO_3): 1479, 1383, 1313, 1187, 711 cm^{-1}. λ_{max} (nm): 287, 330 cm^{-1}. Λ_m (S cm^2 mol^{-1}): 77.2. Thermal analyses: $T_{Decomp.}$ (°C): 298, 307, 647. Residue Calcd. (%) 14.84 (14.93). Anal Calcd. for Dy(III) complex $C_{46}H_{40}N_7O_{21}Dy$ requires: C, 46.45; H, 3.39; N, 8.24; Dy, 13.66; Found: C, 46.54; H, 3.32; N, 8.26; Dy, 13.80. IR ν_{max} (cm^{-1}): ν (C=O): 1609, ν (C=N): 1569, ν (N–H): 3386, ν (NO_3): 1480, 1384, 1316, 1185, 712 cm^{-1}. λ_{max} (nm): 287, 331 cm^{-1}. Λ_m (S cm^2 mol^{-1}): 88.1. Thermal analyses: $T_{Decomp.}$ (°C): 299, 308, 646. Residue Calcd. (%) 15.62 (15.79). Anal Calcd. for Yb(III) complex $C_{46}H_{40}N_7O_{21}Yb$ requires: C, 46.05; H, 3.36; N, 8.17; Yb, 14.42; Found: C, 46.10; H, 3.27; N, 8.25; Yb, 14.39. IR ν_{max} (cm^{-1}): ν (C=O): 1610, ν (C=N): 1571, ν (N–H): 3382, ν (NO_3): 1480, 1383, 1321, 1185, 712 cm^{-1}. λ_{max} (nm): 289, 336 cm^{-1}. Λ_m (S cm^2 mol^{-1}): 73.9. Thermal analyses: $T_{Decomp.}$ (°C): 298, 308, 646. Residue Calcd. (%) 16.21 (16.35). Anal Calcd. for Nd(III) complex $C_{46}H_{40}N_7O_{21}Nd$ requires: C, 47.18; H, 3.44; N, 8.37; Nd, 12.32; Found: C, 47.30; H, 3.38; N, 8.42; Nd, 12.24. IR ν_{max} (cm^{-1}): ν (C=O): 1610, ν (C=N): 1570, ν (N–H): 3390, ν (NO_3): 1479, 1386, 1316, 1184, 709 cm^{-1}. λ_{max} (nm): 291, 343 cm^{-1}. Λ_m (S cm^2 mol^{-1}): 84.9. Thermal analyses: $T_{Decomp.}$ (°C): 298, 308, 646. Residue Calcd. (%) 14.03 (14.20).

4.5. Electronic absorption titration

Electronic absorption titration experiments were performed with fixed concentration drugs (10 μM), while gradually increasing the concentration of CT DNA. When measuring the absorption spectra, an equal amount of CT DNA was added to both the complex solutions and the reference solution to eliminate the absorbance of CT DNA itself. Each sample solution was scanned in the range of 190–500 nm.

4.6. Fluorescence spectra

To compare quantitatively the affinity of the compounds bound to DNA, K_b values of the compounds to DNA were obtained by the luminescence titration method. Fixed amounts of compound were titrated with increasing amounts of DNA, over a range of DNA concentrations from 2.5 to 15 μM. Excitation wave lengths of 331 nm for Nd(III) complex and 323 nm for H_4L were used, and fluorescence emission intensities were monitored at 443 and 440 nm, respectively. The concentration of the bound compound was calculated using equation [44].

$$C_b = C_t[(F - F^0)/(F^{max} - F^0)],$$

where C_t is the total compound concentration, F is the observed fluorescence emission intensity at given DNA concentration, F^0 is the intensity in the absence of DNA, and F^{max} is the fluorescence of the totally bound compound. Binding data were cast into the form of a Scatchard plot of r/C_f versus r, where r is the binding ratio $C_b/[DNA]_t$ and C_f is the free compound concentration. All experiments were conducted at room temperature in a buffer containing 5 mM Tris–HCl (pH 7.1) and 50 mM NaCl concentrations.

Further support for the ligand and complexes binding to DNA via intercalation is given through the emission quenching experiment. EB is a common fluorescent probe for DNA structure and has been employed in the examinations of the mode and process of metal complexes binding to DNA [41]. A 2.0 mL solution of 4 μM DNA and 0.32 μM EB (at saturating binding levels) was titrated by 2.5–35 μM complexes and ligand. Quenching data were analyzed according to the Stern–Volmer equation which could be used to determine the fluorescent quenching mechanism:

$$F_o/F = 1 + K_q[Q],$$

where F_o and F are the fluorescence intensity in the absence and presence of drug at [Q] concentration respectively; K_q is the quenching constant and [Q] is the quencher concentration. Plots of F_o/F versus [Q] appear to be linear and K_q depends on temperature [50].

4.7. Iodide quenching experiments

The fluorescence quenching efficiency is evaluated by Stern–Volmer K_{sv}, which varies with the experimental conditions. The values of K_{sv} were used to deduce the interaction mode of the fluorescence probe with DNA. High binding constants should correspond to better protection by the DNA and a stronger inhibition of quenching by anionic species. Quenching plots were constructed according to the following Stern–Volmer equation.

$$F_o/F = 1 + K_{sv}[I^-],$$

where F_o and F are the fluorescence intensity in the absence and presence of iodide at [I^-] concentration, respectively; K_{sv} is the quenching constant and [I^-] is the concentration of iodide. Plots of F_o/F versus [I^-] appear to be linear and K_{sv} was evaluated by linear least-squares analysis of the data according to the equation [51].

4.8. Salt effect

Fluorescence intensities were recorded in the absence and presence of DNA in the mixture solution of each compound and NaCl at room temperature.

4.9. Viscosity measurements

Viscosity experiments were conducted on an Ubbelohde viscometer, immersed in a thermostated water bath maintained to 25.0 °C. Titrations were performed for the complexes (0.5–4 μM), and each compound was introduced into a DNA solution (5 μM) present in the viscometer. Data were presented as $(\eta/\eta_0)^{1/3}$ versus the ratio of the concentration of the compound and DNA, where η is the viscosity of DNA in the presence of the compound and η_0 is the viscosity of DNA alone [52,53].

4.10. Antioxidant activity

In antioxidant activity experiments the superoxide radicals ($O_2^{-\bullet}$) were produced by the system MET/VitB_2/NBT [54]. The amount of $O_2^{-\bullet}$ and suppression ratio for $O_2^{-\bullet}$ can be calculated by measuring the absorbance at 560 nm, because NBT can be reduced quantitatively to blue formazan by $O_2^{-\bullet}$. The solution of MET, VitB_2 and NBT was prepared with 0.067 M phosphate buffer (pH = 7.8) at the condition of avoiding light. The tested compounds were dissolved in DMF. The reaction mixture contained MET (0.01 mol L^{-1}), NBT (4.6×10^{-5} mol L^{-1}), VitB_2 (3.3×10^{-6} mol L^{-1}), phosphate buffer solution (0.067 mol L^{-1}) and the tested compound (the final concentration: $C_{i(i=1-6)}$ = 0.4, 1.0, 2.0, 4.0, 6.0, 8.0 μM). After incubating at 30 °C for 10 min and illuminating with a fluorescent lamp for 3 min, the absorbance (A_i) of the samples was measured at 560 nm. The sample without the tested compound and avoiding light was used as the control. The suppression ratio for $O_2^{-\bullet}$ was calculated from the following expression:

$$\text{Suppression ratio}(\%) = [(A_0 - A_i)/A_0] \times 100\%$$

where A_i = the absorbance in the presence of the ligand or its complexes, A_0 = the absorbance in the absence of the ligand or its complexes.

In antioxidant activity experiments the hydroxyl radical ($HO^\bullet$) in aqueous media was generated through the Fenton reaction [55]. The solution of the tested compounds was prepared with DMF. The reaction mixture contained 2.5 mL 0.15 M phosphate buffer (pH = 7.4), 0.5 mL 114 μM safranin, 1 mL 945 μM EDTA–Fe(II), 1 mL 3% H_2O_2 and 30 μL the tested compound solution (the final concentration: $C_{i(i=1-6)}$ = 1.0, 2.0, 3.0, 4.0, 5.0, 6.0 μM). The sample without the tested compound was used as the control. The reaction mixtures were incubated at 37 °C for 60 min in a water bath. Absorbances (A_i, A_0, A_c) at 520 nm were measured. The suppression ratio for $HO^\bullet$ was calculated from the following expression:

$$\text{Suppression ratio}(\%) = [(A_i - A_0)/(A_c - A_0)] \times 100\%$$

where A_i = the absorbance in the presence of the tested compound; A_0 = the absorbance in the absence of the tested compound; A_c = the absorbance in the absence of the tested compounds, EDTA–Fe(II) and H_2O_2.

The antioxidant activity was expressed as the 50% inhibitory concentration (IC_{50}). IC_{50} values were calculated from regression lines where: x was the tested compound concentration in μM and y was percent inhibition of the tested compounds.

Acknowledgements

This work is supported by the National Natural Science Foundation of China (20475023) and Gansu NSF (0710RJZA012).

References

[1] E.C. Miller, J.A. Miller, Cancer 47 (1981) 1055–1064.
[2] A.E. Friedman, C.V. Kumar, N.J. Turro, J.K. Barton, Nucleic Acids Res. 19 (1991) 2595–2602.
[3] A.M. Pyle, T. Morri, J.K. Barton, J. Am. Chem. Soc. 112 (1990) 9432–9434.
[4] J.K. Barton, J.M. Goldberg, C.V. Kumar, N.J. Turro, J. Am. Chem. Soc. 108 (1986) 2081–2088.
[5] P.H. Proctor, E.S. Reynolds, Physiol. Chem. Phys. Med. NMR 16 (1984) 175–195.
[6] K.E. Erkkila, D.T. Odom, J.K. Barton, Chem. Rev. 99 (1999) 2777–2795.
[7] M. Mrksich, P.B. Dervan, J. Am. Chem. Soc. 115 (1993) 9892–9899.
[8] B.N. Trawick, A.T. Danihe, J.K. Bashkin, Chem. Rev. 98 (1998) 939–960.
[9] K. Dhara, J. Ratha, M. Manassero, X.Y. Wang, S. Gao, P. Banerjee, J. Inorg. Biochem. 101 (2006) 95–103.
[10] D.M. Kong, J. Wang, L.N. Zhu, Y.W. Jin, X.Z. Li, H.X. Shen, H.F. Mi, J. Inorg. Biochem. 102 (2008) 824–832.
[11] F. Firdaus, K. Fatma, M. Azam, S.N. Khan, A.U. Khan, M. Shakir, Transition Met. Chem. 33 (2008) 467–473.
[12] B.K. Kaymakcioglu, S. Rollas, Farmaco 57 (2002) 595–599.
[13] S. Küçükgüzel, S. Rollas, I. Küçükgüzel, M. Kiraz, Eur. J. Med. Chem. 34 (1999) 1093–1100.
[14] S.R. Zhang, A.D. Sherry, J. Solid State Chem. 171 (2003) 38–43.
[15] Z.Y. Yang, Synth. React. Inorg. Met.-Org. Chem. 30 (2000) 1265–1272.
[16] B.D. Wang, Z.Y. Yang, Q. Wang, T.K. Cai, P. Crewdson, Bioorg. Med. Chem. 14 (2006) 1880–1888.
[17] B.D. Wang, Z.Y. Yang, D.D. Qin, Z.N. Chen, J. Photochem. Photobiol., A: Chem. 194 (2008) 49–58.
[18] B.D. Wang, Z.Y. Yang, T.R. Li, Bioorg. Med. Chem. 14 (2006) 6012–6021.
[19] F. Yakuphanoglu, M. Sekerci, J. Mol. Struct. 751 (2005) 200–203.
[20] T. Miyadera, E.M. Kosower, J. Med. Chem. 15 (1972) 339–340.
[21] J.V. Formica, W. Regelson, Food Chem. Toxicol. 33 (1995) 1061–1080.
[22] Y.Z. Cai, Q. Luo, M. Sun, H. Corke, Life Sci. 74 (2004) 2157–2184.
[23] K.E. Heim, A.R. Tagliaferro, D.J. Bobilya, J. Nutr. Biochem. 13 (2002) 572–584.
[24] H.C. Cooray, T. Janvilisri, H.W. Veen, S.B. Hladky, M.A. Barrand, Biochem. Biophys. Res. Commun. 317 (2004) 269–275.
[25] F.V. So, N. Guthrie, A.F. Chambers, K.K. Carroll, Cancer Lett. 112 (1997) 127–133.
[26] Y. Mitsunaga, H. Takanaga, H. Matsuo, M. Naito, T. Tsuruo, H. Ohtani, Y. Sawada, Eur. J. Pharmacol. 395 (2000) 193–201.
[27] K.A. Youdim, M.S. Dobbie, G. Kuhnle, A.R. Proteggente, N.J. Abbott, C. Rice-Evans, J. Neurochem. 85 (2003) 180–192.
[28] J.O. Jim, J. Brown, J. Fleming, P.R. Harrison, Biochem. Pharmacol. 66 (2003) 2075–2088.
[29] I. Kostova, N. Trendafilova, G. Momekov, J. Trace Elem. Med. Biol. 22 (2008) 100–111.
[30] C.C. Bisi, O. Carugo, Inorg. Chim. Acta 159 (1989) 157–161.
[31] D.Z. Horne, P.B. Dervan, J. Am. Chem. Soc. 112 (1990) 2435–2437.
[32] J.M. Gottesfield, L. Nealy, J.W. Trauger, E.E. Baird, P.B. Dervan, Nature 387 (1997) 202–205.
[33] W.J. Geary, Coord. Chem. Rev. 7 (1971) 81–122.
[34] F. Maarchetti, C. Pettinari, R. Pettinari, D. Leonesi, A. Lorenzotti, Polyhedron 18 (1999) 3041–3050.
[35] K. Narang, V.P. Singh, Transition Met. Chem. 18 (1993) 287–290.

[36] B.D. Wang, Z.Y. Yang, D.W. Zhang, Y. Wang, Spectrochim. Acta, Part A 63 (2006) 213–219.
[37] J.K. Barton, A. Danishefsky, J. Goldberg, J. Am. Chem. Soc. 106 (1984) 2172–2176.
[38] J.G. Liu, Q.L. Zhang, X.F. Shi, L.N. Ji, Inorg. Chem. 40 (2001) 5045–5050.
[39] W.D. Wilson, L. Ratmeyer, M. Zhao, L. Stekowshi, D. Boykin, Biochemistry 32 (1993) 4098–4104.
[40] H. Xu, K.C. Zheng, L.J. Lin, H. Li, Y. Gao, L.N. Ji, Inorg. Chem. 98 (2004) 87–97.
[41] Y.B. Zeng, N. Yang, W.S. Liu, N. Tang, J. Inorg. Biochem. 97 (2003) 258–264.
[42] C.V. Kumar, J.K. Barton, N.J. Turro, J. Am. Chem. Soc. 107 (1985) 5518–5523.
[43] L.S. Lerman, J. Mol. Biol. 3 (1961) 18–30.
[44] G.M. Howe, K.C. Wu, W.R. Bauer, Biochemistry 15 (1976) 4339–4346.
[45] S. Satyanarayana, J.C. Dabrowiak, J.B. Chaires, Biochemistry 32 (1993) 2573–2584.
[46] J.G. Liu, B.H. Ye, H. Li, Q.X. Zhen, L.N. Ji, Y.H. Fu, J. Inorg. Biochem. 76 (1999) 265–271.
[47] S.S. Leonard, D. Keil, T. Mehlmanb, S. Proper, X. Shi, G.K. Harris, J. Ethnopharmacol. 103 (2006) 288–296.
[48] R.G. Xing, H.H. Yu, S. Liu, W.W. Zhang, Q.B. Zhang, Z.E. Li, P.C. Li, Bioorg. Med. Chem. 13 (2005) 1387–1392.
[49] Z.Y. Yang, X.H. Xu, R.D. Yang, Q. Li, J. Rare Earths 13 (1995) 89–93.
[50] M.R. Efink, C.A. Ghiron, Anal. Biochem. 114 (1981) 199–206.
[51] C.V. Kumar, R.S. Turner, E.H. Asuncion, J. Photochem. Photobiol., A: Chem. 74 (1993) 231–238.
[52] M. Eriksson, M. Leijon, C. Hiort, B. Norden, A. Gradsland, Biochemistry 33 (1994) 5031–5040.
[53] Y. Xiong, X.F. He, X.H. Zou, J.Z. Wu, X.M. Chen, L.N. Ji, R.H. Li, J.Y. Zhou, R.B. Yu, J. Chem. Soc., Dalton Trans. 1 (1999) 19–24.
[54] C.C. Winterbourn, Biochem. J. 182 (1979) 625–628.
[55] C.C. Winterbourn, Biochem. J. 198 (1981) 125–131.